Evidence of Regulating Effect of Nitrogen Level on Ultramicrostructure and Mapping Elements of Tomato (*Lycopersiconesculentum* Mill.) Chloroplast under Heat Stress

Chunying Li , Zaiqiang Yang , Chunlong Zhang * , Jing Luo , Di Wang , Yehan Yan

Posted Date: 18 January 2024

doi: 10.20944/preprints202401.1427.v1

Keywords: heat stress; nitrogen levels; TEM-EDX mapping; chloroplast; tomato (*Lycopersiconesculentum* Mill.)

Article

Evidence of Regulating Effect of Nitrogen Level on Ultramicrostructure and Mapping Elements of Tomato (*Lycopersiconesculentum* Mill.) Chloroplast under Heat Stress

Chunying Li [1,2], Zaiqiang Yang [2], Chunlong Zhang [3,*], Jing Luo [2], Di Wang [4] and Yehan Yan [1]

[1] School of Environment and Tourism, West Anhui University, Lu'an, 237000, China; 20211108008@nuist.edu.cn; yanyh@mail.ustc.edu.cn

[2] School of Ecology and Applied Meteorology, Nanjing University of Information Science & Technology; Nanjing, 210044,China; 20211108008@nuist.edu.cn (C.L.); yzq@nuist.edu.cn (Z.Y.); 20211208035@nuist.edu.cn (J.L.);

[3] School of Electrical and Optoelectronic Engineering, West Anhui University, Lu'an, 237000, China; 42000017@wxc.edu.cn (C.Z.);

[4] Liaoning meteorological service center, Shenyang, 110001, China; Wangdi_lnqx@163.com

* Correspondence: 42000017@wxc.edu.cn; Tel.: +86-13624602249

Abstract: Heat stress is a serious threat to tomato production. The ultrastructure and element mapping of tomato chloroplast were investigated under different nitrogen levels to explore the regulatory effect of nitrogen on tomato chloroplast under heat stress. Experiments design two temperature treatments (25°C/15°C, as control, 40°C/30°C, as severe high-temperature, SHT) and four nitrogen levels (0.0 kg hm^{-2}, N1; 187.5 kg hm^{-2}, N2; 250 kg hm^{-2}, N3, as recommended nitrogen-application; 312.5kg hm^{-2} , N4) for a duration of 5 days in artificial climate chamber. The results showed that heat stress led to obvious damage to the ultrastructure of tomato chloroplast, including thylakoid stacking disorder, granum destruction, and starch grain aggregation and degradation. With the increase of nitrogen level, the ratio of long and short axes of tomato chloroplasts increased, the differentiation of chloroplasts was strengthened, the number of plastoglobuli was increased and aggregated, and the degree of damage to the ultrastructure of chloroplasts was reduced. Element mapping analysis revealed that heat stress significantly increased the contents of calcium, phosphorus and chlorine in the chloroplast of tomato leaves, while the contents of potassium was decreased. The application of nitrogen fertilizer could significantly regulate the element distribution of tomato chloroplast under heat stress, especially the regulation of phosphorus, chlorine, calcium, magnesium. These results provide new insight into the role of nitrogen using TEM-EDX mapping in the protection of tomato chloroplast under heat stress and the mechanism of heat stress tolerance in plants.

Keywords: heat stress ; nitrogen levels; TEM-EDX mapping; chloroplast; tomato (*Lycopersiconesculentum* Mill.)

1. Introduction

With increasing global warming, heat stress has become one of the most important abiotic stresses affecting tomato yield and quality [1]. Heat stress inhibits the growth and development of tomato, resulting in dwarf plants, smaller leaves, and poor root development [2,3]. High temperatures also cause damage to the chloroplast structure of tomato leaves, thereby reducing the efficiency of photosynthesis [4]. Photosynthesis is a key process in plant growth and yield formation, so inhibition of photosynthesis can negatively affect tomato growth and yield. With the rapid development of bioelectron microscopy technology, changes in the internal structure of chloroplasts can be directly observed by high-resolution transmission electron microscopy (TEM, resolution at the micron to nanometre scale).

Nitrogen is one of the essential nutrients for plant growth and has an important effect on growth and development, photosynthesis and stress resistance [5,6]. Chloroplasts are the site of photosynthesis and an important organ for nitrogen metabolism in plants. In chloroplasts, nitrogen

 doi:10.20944/preprints202401.1427.v1

is involved in the synthesis of chlorophyll, proteins, nucleic acids and other important substances [7–10]. Chlorophyll is the key pigment for photosynthesis in plants, and its synthesis requires the participation of nitrogen. Proteins are the components of various enzymes, receptors and other important molecules in chloroplasts, and nitrogen is the main component of proteins. Chloroplasts are organelles that content their own genomes ,which encode key genes for carbon dioxide fixation. Nucleic acids, which are carriers of genetic information, also play an important role in chloroplasts, and nitrogen is also one of the important constituent elements of nucleic acids. Therefore, nitrogen levels are critical to the structure and function of chloroplasts.

Many physiological and horticultural studies have shown that proper application of nitrogen fertiliser at high temperatures can alleviate the damage caused by high temperatures to plants. Under heat stress, moderate nitrogen supply can promote the growth and development of tomato, and improve the indicators of plant height, stem thickness, number of leaves and leaf area [11,12]. Appropriate supply of nitrogen can increase the photosynthetic rate and the accumulation of photosynthetic products in tomato [13]. Under heat stress, either too high or too low a nitrogen level reduces tomato's stress tolerance, making it more susceptible to heat injury and pest and disease attack. Additionally, Nitrogen is related to the synthesis of chlorophyll. When nitrogen is sufficient, plants synthesize more proteins, which promotes cell division and growth, so the plant's leaf area grows faster and more leaf area can be used for photosynthesis [14]. Therefore, in order to improve the adaptability and yield of tomato under heat stress, the level of nitrogen supply needs to be rationally controlled. The specific nitrogen supply level needs to be considered and adjusted according to soil fertility, climatic conditions, variety characteristics and cultivation management.

Photosynthesis is one of the most sensitive biological processes to heat stress in plant. The photosynthesis system in chloroplasts is contained in an extended thylakoid (cyst-like) membrane system. In young leaves, developing chloroplasts also contain numerous plastid spheres and thylakoid-associated liposomes [15]. The electron transport chain in the thylakoid membrane system in chloroplasts captures light energy and produces NADPH, as well as a transmembrane proton gradient that drives ATP synthesis. In turn, NADPH and ATP provide energy for photosynthetic fixation in the chloroplast stroma. Chloroplasts contain two distinct endomembrane regions-stacked thylakoids [stroma (grana); singular granum] and unstacked stroma thylakoids (stroma thylakoid), which form a continuous network enclosing a single associative (branching and reconnecting) chamber-the thylakoid lumen [16–18]. The number of thylakoids in a mature chloroplast stroma is variable, ranging from a few to more than 40, depending on the plant species and environment. Typically, plants grown in the shade contain more numerous and thicker basidia than individuals of the same species grown in the light. Non-stacked basidiomycetes differ from stacked basidiomycetes in many important ways. For example, photosystem I and the ATP synthase complex are present only in the unstacked regions of the matrix vesicles and the stacked basal granules. Photosystem II and light-trapping complex II, on the other hand, are found primarily in the adherent regions of the stacked vesicles [19]. This segregation of protein complexes between membranes on the adherent side of the stacked region and membranes on the unfastened side of the unstacked region is called lateral heterogeneity of the photosynthetic membrane system [20–22]. The vesicle-like stacking structure is common in green plants and is thought to be involved in regulating the partitioning of absorbed light energy between photosystem I and photosystem II in photosynthesis. plastoglobuli are lipoproteasomes formed by a single layer of polar lipids surrounded and attached to the stromal side of the cystoid membrane. The lipid cores contain various types of isoprenylbenzoquinones [α-tocopherol (vitamin E), chlorophyll quinone (vitamin K1), plastoquinone, and methylnaphthoquinone], as well as the degradation products of carotenoids, neutral lipids, and chlorophyll. The boundary layer is composed of a monolayer of galectin glycerol, structural proteins called plastoglobulins, and enzymes involved in the synthesis and metabolism of core lipids. The size and number of plastoglobulins change during plastid development and differentiation; the number of plastoglobulins becomes larger in response to environmental stresses (e.g., intense light, drought, high salt and high ozone environments) and during senescence [23]. Morphological changes in chloroplasts under high temperature stress can be an important indicator for evaluating heat

 doi:10.20944/preprints202401.1427.v1

tolerance in tomato at the cellular level. The microstructure of chloroplasts changes under heat stress, and understanding these changes can help to understand the response and adaptation mechanisms of plants to heat stress, as well as to screen and breed heat-tolerant varieties.

Green plants are the only multicellular autotrophic organisms that can take up inorganic elements from the environment without relying on energetic compounds synthesized by other organisms. Chloroplasts are composed of a variety of elements and compounds. Either quantitatively or qualitatively resolving the elemental composition of chloroplasts is important for analysing the molecular structure, transport mechanisms and processes of various substances in chloroplasts [24–26]. Currently, physiology can resolve the mechanisms of transport and utilization of mineral ion nutrition at the plant tissue level, but it cannot deeply resolve individual transport mechanisms. With the application of molecular techniques, whole genome sequencing, the development of model plant systems, high-resolution electrophysiological methods [27], and other sophisticated means of studying plant physiology, it has become possible to reveal the mechanisms of mineral nutrient transport and utilization at the molecular level.

The main objective of this study was to determine the ultramicrostructure and mapping elements of tomato leaves chloroplast to provide basic data and methods for further research on photosystem activity and molecular regulatory mechanisms under heat stress. Meanwhile, based on the physiological studies of tomato under different heat stresses by nitrogen application levels, this study attempted to explain the response mechanism of the differences in photosystem activity and photosynthetic capacity of tomato leaves to nitrogen levels under high temperature stress, based on the analysis of the quantitative localization of various submicroscopic structural parameters and constituent elements of chloroplasts. Therefore, this study provides support for nitrogen application under high temperature environment in tomato production.

2. Results

2.1. Ultrastructures of choroplasts in tomato leaves

The chloroplasts were dispersed and arranged close to the cell wall under N1 treatment at room temperature, and the chloroplasts were rounded with an area between 74.9540 μm^2 and 7.3291 μm^2(Figure 1). The starch granules in chloroplasts accounted for between 28% and 49% of the area of the stroma, and the rest of the chloroplasts were semi-crystalline structures. Plastids were mainly distributed in the chloroplast stroma, and plastoglobuli were small in area and ranged from 3 to 13 in number. The number of stromal vesicles ranged from 7 to 15, the number of layers of stromal vesicles ranged from 9 to 19, and the thickness of stromal vesicles ranged from 0.18 μm to 0.45 μm. The area of the vesicles ranged from 60.1324 μm^2 to 91.2688 μm^2.The thickness of the chloroplast bilayer periplasm ranged from 0.06 to 0.11 μm. The thickness of the cell wall of the spongy tissue chloroplasts ranged between 0.04-0.08 μm.

 doi:10.20944/preprints202401.1427.v1

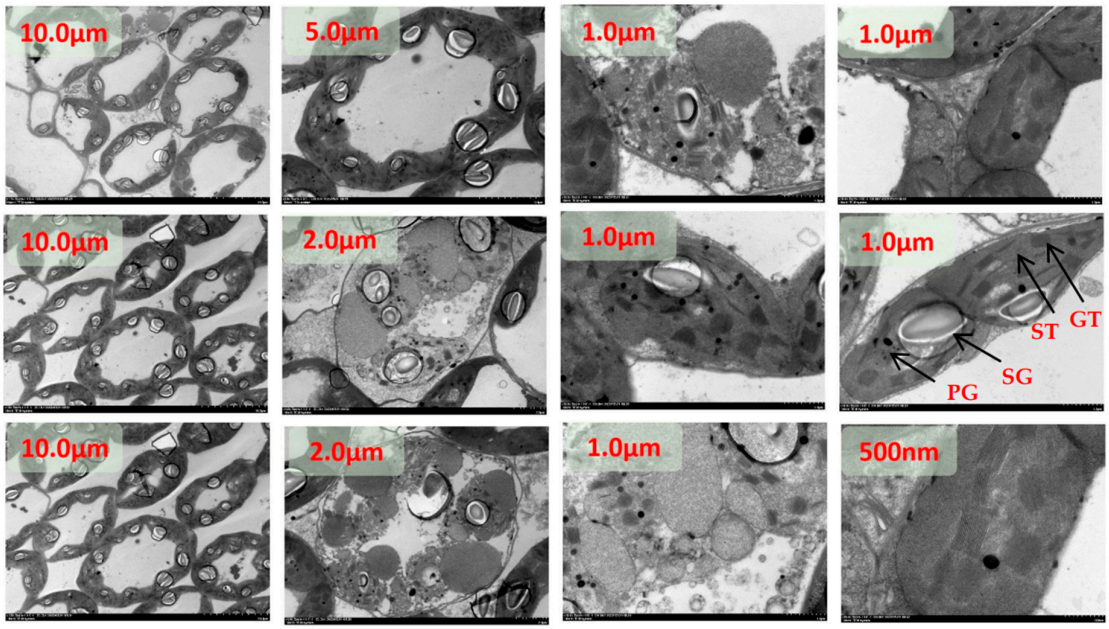

Figure 1. Chloroplast ultrastructure of tomato leaves under day/night temperature 25 °C/15 °C with N1 treatment . SG, starch grains; PG, plastoglobuli; GT, grana thylakoid; ST,stroma thylakoid.

Under low N2 treatment at room temperature, some chloroplasts were dispersed and arranged close to the cell wall, and some chloroplasts left the cell wall and dispersed to the center of the cell(Figure 2). The chloroplasts were rounded and ranged in area from 2.8381 μm² to 18.3863 μm². Starch grains in chloroplasts accounted for between 60% and 83% of the area of amyloplasts, and the area of semi-crystalline structures was significantly reduced compared with the N1 treatment. plastoglobuli were mainly distributed in the chloroplast stroma, and the area of plastoglobuli slivered N1 to become larger, with the number of microspheres ranging from four to eight. The number of basal vesicles ranged from 8 to 16, the number of layers of basal vesicles ranged from 12 to 20, and the thickness of basal vesicles ranged from 0.22 μm to 0.46 μm. The cell area increased from N1, with an area between 136.1321 μm² and 159.6235 μm². Vesicle area ranged from 70.5062 μm² to 98.7598 μm². The thickness of the chloroplast bilayer periplasm ranged from 0.08 to 0.12 μm. The thickness of the cell wall of the sponge tissue chloroplasts ranged from 0.05-0.09 μm.

Preprints (www.preprints.org) | NOT PEER-REVIEWED | Posted: 18 January 2024 doi:10.20944/preprints202401.1427.v1

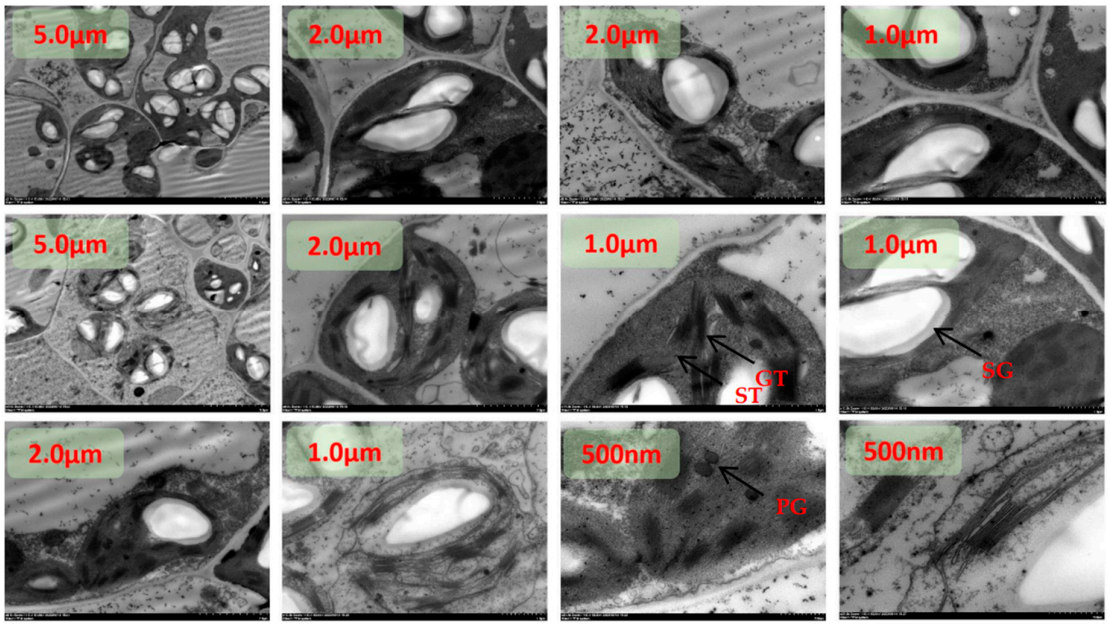

Figure 2. Chloroplast ultrastructure of tomato leaves under day/night temperature 25 °C/15 °C with N2 treatment. SG, starch grains; PG, plastoglobuli; GT, grana thylakoid; ST,stroma thylakoid.

The chloroplasts were dispersed and arranged close to the cell wall and most of the chloroplasts were distributed close to the cell wall under the recommended nitrogen application rate N3 treatment at room temperature(Figure 3). The degree of chloroplast differentiation increased, the distance ratio between the long and short axes became smaller, and the ends became pointed. The chloroplast area ranged from 4.4701 μm² to 26.0546 μm². Starch granules in chloroplasts accounted for between 40% and 67% of the amyloplast area, and the surface of the starch granules was surrounded by a conspicuous oleaginous substance. plastoglobuli were mainly distributed in the chloroplast stroma, close to one end of the stroma-like vesicle. plastoglobuli became larger in area than N1 and ranged in number from four to nine. The number of stromal vesicles ranged from 5 to 22, the number of layers of stromal vesicles ranged from 25 to 38, and the thickness of stromal vesicles ranged from 0.25 μm to 0.65 μm. The cell area increased from N1, with an area between 122.3671 μm² and 225.0059 μm². Vesicle area ranged from 45.5062 μm² to 98.7598 μm². The thickness of the chloroplast bilayer periplasm ranged from 0.08 to 0.16 μm. The thickness of the cell wall of the sponge tissue chloroplasts ranged between 0.06-0.10 μm.

Preprints (www.preprints.org) | NOT PEER-REVIEWED | Posted: 18 January 2024 doi:10.20944/preprints202401.1427.v1

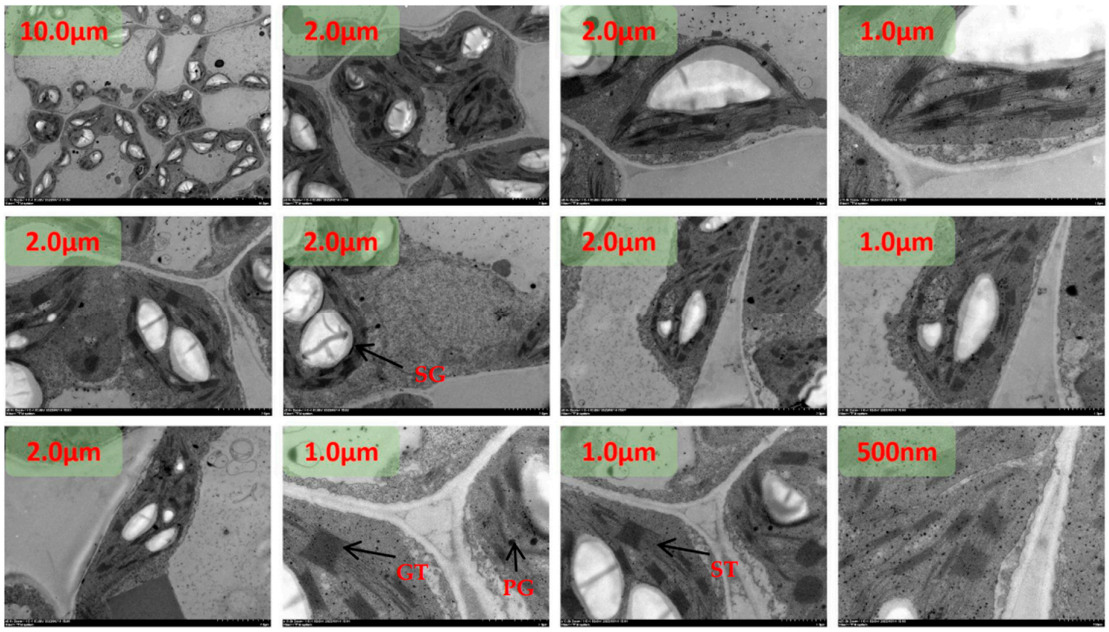

Figure 3. TEM images of tomato chloroplasts under day/night temperature 25 °C/15 °C with N3 treatment. SG, starch grains; PG, plastoglobuli; GT, grana thylakoid; ST,stroma thylakoid.

At room temperature, the chloroplasts were partly dispersed close to the cell wall and partly in the center of the cell under high dan N4 treatment(Figure 4). The chloroplasts were morphologically dispersed and structurally scattered, and the distance ratio between the long and short axes increased. The chloroplast area ranged from 3.0649 μm^2 to 10.9326 μm^2. The starch granules in chloroplasts accounted for between 20% and 43% of the amyloplast area, and the amyloplasts were differentiated from the middle, with the surface of the amyloplasts clearly surrounded by fluid. Plastid spherules were mainly distributed in the chloroplast stroma, partly in close proximity to one end of the stroma-like vesicle. plastoglobuli are small in size and range in number from two to six. The number of basal granule-like vesicles ranged from 10 to 17, the number of layers of basal granule-like vesicles ranged from 21 to 47, and the thickness of basal granule-like vesicles ranged from 0.21 μm to 0.56 μm. The cell area was significantly reduced from N3, with the area ranging from 62.4617 μm^2 to 143.6653 μm^2. Vesicle area ranged from 21.1290 μm^2 to 97.1640 μm^2. The thickness of the chloroplast bilayer periplasm ranged from 0.06 to 0.18 μm. The thickness of the cell walls of the sponge tissue chloroplasts ranged between 0.07-0.13 μm.

 doi:10.20944/preprints202401.1427.v1

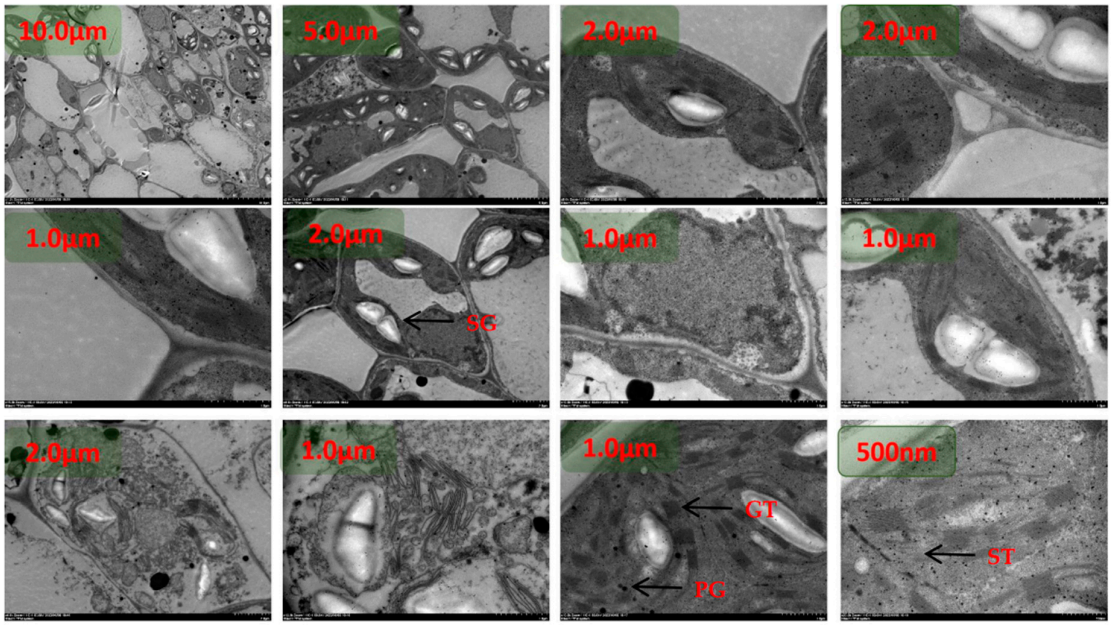

Figure 4. TEM images of tomato chloroplasts under day/night temperature 25 °C/15 °C with N4 treatment. SG, starch grains; PG, plastoglobuli; GT, grana thylakoid; ST,stroma thylakoid.

Under heat stress, chloroplasts were dispersed and arranged close to the cell wall under N1 treatment(Figure 5). The morphological structure of chloroplasts was scattered and more rounded, and the distance between the long and short axes was significantly larger than that of the ambient temperature treated group. The number of chloroplasts was significantly reduced, with the number ranging from 0-4. The chloroplast area ranged from 2.7240 μm² to 10.6230 μm². There were no starch grains in the chloroplasts. The number of stromal vesicles was significantly increased, with values ranging from 3 to 13, aggregated, more two or three aggregates, mostly distributed in the middle constriction of the chloroplasts at the tip of that of the differentiation, with a clear directionality of movement. A few were translocated to the outside of the cell. The basidiomycetes were disorganized, with the number of individuals ranging from 11 to 21, the number of layers of basidiomycetes ranging from 32 to 40, and the thickness of basidiomycetes ranging from 0.39 μm to 0.46 μm. The cell area was significantly reduced compared to the normothermic control, with areas ranging from 36.3457 μm² to 79.8773 μm². Vesicle area ranged from 18.4497 μm² to 47.7753 μm². The thickness of the chloroplast bilayer periplasm ranged from 0.06 to 0.18 μm. The thickness of the cell wall of the sponge tissue chloroplasts ranged between 0.0-0.09 μm.

Preprints (www.preprints.org) | NOT PEER-REVIEWED | Posted: 18 January 2024 doi:10.20944/preprints202401.1427.v1

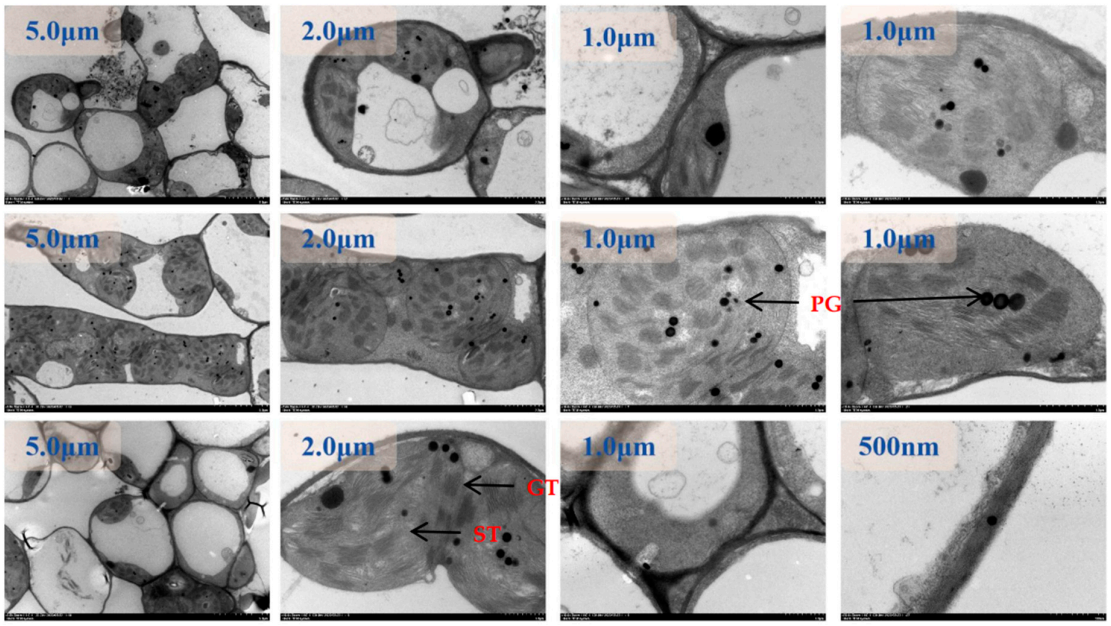

Figure 5. TEM images of tomato chloroplasts under day/night temperature 40 °C/30 °C with N1 treatment. SG, starch grains; PG, plastoglobuli; GT, grana thylakoid; ST,stroma thylakoid.

Under heat stress, the chloroplasts were dispersed and arranged close to the cell wall under low N2 treatment(Figure 6). The morphological structure of chloroplasts was clearer, pointed at both ends, and some chloroplasts were in the differentiation stage. The distance ratio between the long and short axes of chloroplasts was about 2-3, which was significantly larger than that of HTN1 treatment. The number of chloroplasts was between 2-5. Chloroplast area ranged from 5.3997 μm² to 16.7893 μm². There were starch granules in the chloroplasts, and the area of starch granules accounted for 7-30% of the chloroplast area. The number of plastoglobuli was significantly reduced compared to HTN1, with values ranging from 2 to 8, and was distributed in the chloroplast matrix, close to the side of the stroma-like vesicle. The basidiomycetes were regularly arranged, with the number of individuals ranging from 13 to 22, the number of layers of basidiomycetes ranging from 14 to 32, and the thickness of basidiomycetes ranging from 0.21 μm to 0.46 μm. There was a significant increase in cell area HTN1, which ranged from 87.3381 μm² to 104.8773 μm². Vesicle area ranged from 21.2568 μm² to 56.3314 μm². The thickness of the chloroplast bilayer periplasm ranged from 0.07 to 0.19 μm. The thickness of the cell wall of the spongy tissue chloroplasts ranged between 0.13-0.19 μm.

 doi:10.20944/preprints202401.1427.v1

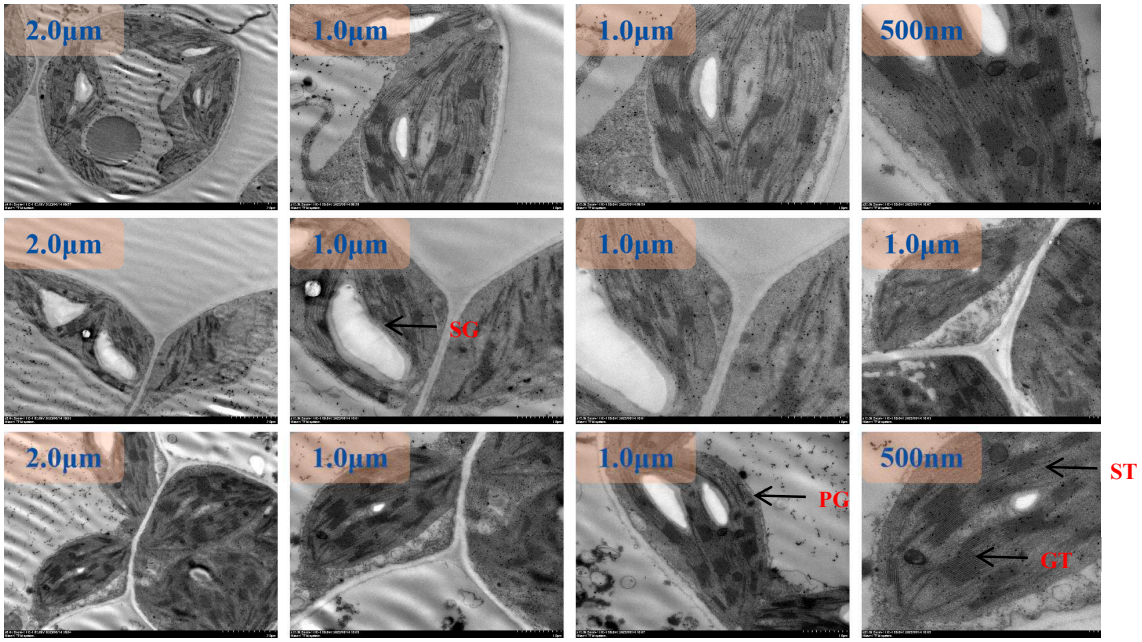

Figure 6. TEM images of tomato chloroplasts under day/night temperature 40 °C/30 °C with N2 treatment. SG, starch grains; PG, plastoglobuli; GT, grana thylakoid; ST,stroma thylakoid .

Under heat stress, the chloroplasts were dispersed close to the cell wall under the recommended N3 treatment(Figure 7). The morphological structure of chloroplasts was clearer, pointed at both ends, and some chloroplasts were in the differentiation stage. The distance ratio between the long and short axes of chloroplasts increased. The number of chloroplasts ranged from 2 to 5. The area of chloroplasts ranged from 2.9035 μm² to 16.5264 μm². There were starch granules in the chloroplasts and the area of starch granules was 41%-70% of the chloroplast area. The number of plastoglobuli was small, with values ranging from two to four. The basidiomycetes were arranged in a pike-like pattern, with the number of individuals ranging from 8 to 21, the number of layers of basidiomycetes ranging from 25 to 30, and the thickness of the basidiomycetes ranging from 0.17 μm to 0.45 μm. There was a significant increase in cell area HTN1, which ranged from 86.2645 μm² to 106.3349 μm². Vesicle area ranged from 20.8660 μm² to 45.4991 μm². The thickness of the chloroplast bilayer periplasm ranged from 0.07 to 0.1 μm. The thickness of the cell wall of the sponge tissue chloroplasts ranged from 0.14-0.25 μm.

Preprints (www.preprints.org) | NOT PEER-REVIEWED | Posted: 18 January 2024 doi:10.20944/preprints202401.1427.v1

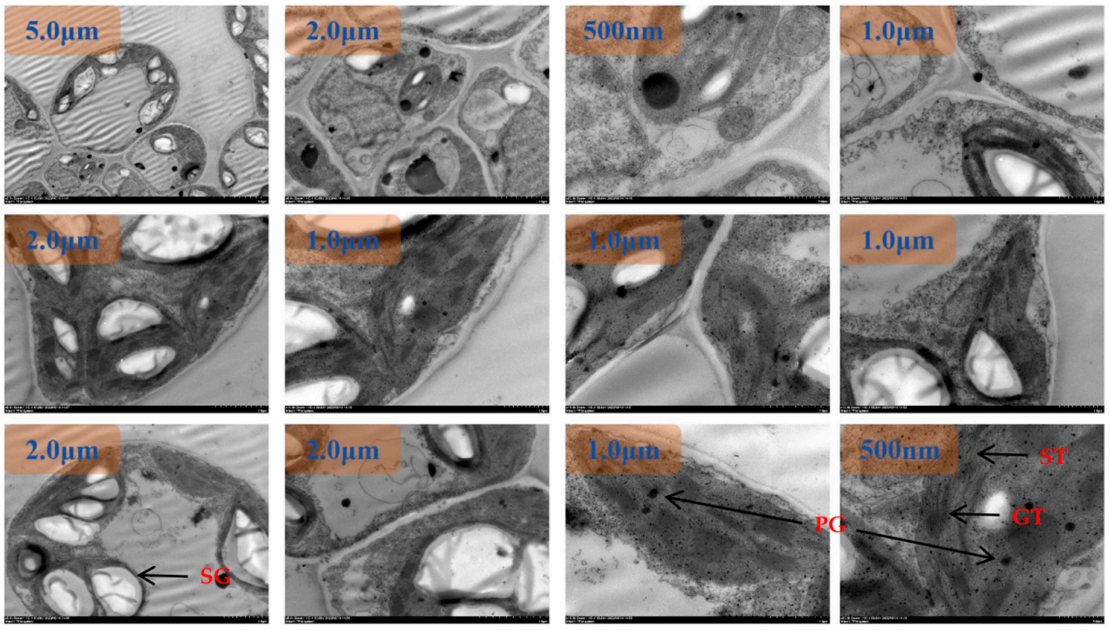

Figure 7. TEM images of tomato chloroplasts under day/night temperature 40 °C/30 °C with N3 treatment. SG, starch grains; PG, plastoglobuli; GT, grana thylakoid; ST,stroma thylakoid.

Under heat stress and high nitrogen N4 treatment, chloroplast morphology and structure became blurred, pointed at both ends, and some chloroplasts were in the differentiation stage(Figure 8). The distance ratio between the long and short axes of chloroplasts increased. The number of chloroplasts ranged from 2-4. The area of chloroplasts ranged from 3.4560 μm² to 9.5971 μm². There were a few starch granules in the chloroplasts and the area of starch granules was 1-15% of the chloroplast area. The number of plastoglobuli was small, with values ranging from two to four. The basidiomycetes were arranged in a pike-like pattern, with the number of individuals ranging from 9 to 26, the number of layers of basidiomycetes ranging from 23 to 28, and the thickness of basidiomycetes ranging from 0.17 μm to 0.45 μm. The cell area was between 97.5207 μm² and 121.9598 μm². Vesicle area ranged from 40.3326 μm² to 79.7893 μm². The thickness of the chloroplast bilayer periplasm ranged from 0.05 to 0.11 μm. The thickness of the cell wall of the sponge tissue chloroplasts ranged between 0.10-0.16 μm.

Preprints (www.preprints.org) | NOT PEER-REVIEWED | Posted: 18 January 2024 doi:10.20944/preprints202401.1427.v1

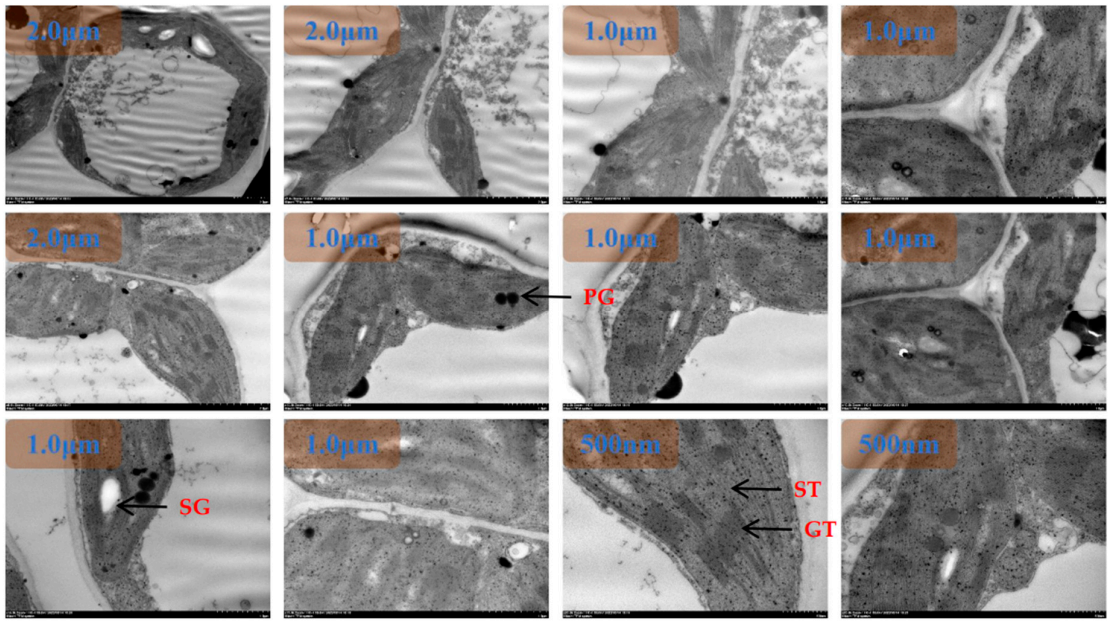

Figure 8. TEM images of tomato chloroplasts under day/night temperature 40 °C/30 °C with N4 treatment. SG, starch grains; PG, plastoglobuli; GT, grana thylakoid; ST,stroma thylakoid.

2.2. Elements distribution of tomato leaves chloroplast under heat stress

The distribution of elements in chloroplasts under control and high-temperature treatments was shown by TEM-EDX Mapping analysis (Figures 9–12). The main distribution of elements were C, N, O, P, Cl, and Mg in chloroplasts under the control condition (CKTN3), the elements P and Cl were enriched in chloroplasts and the chloroplast boundaries could be outlined, as well as the inner chloroplasts of the grana and stroma thylakoid could be distinguished from the amyloplast and the elaioplast structures(Figure 9). Small amounts of Mg and Ca elements were distributed on both grana and stroma thylakoid structures. The most abundant elements analyzed by quantitative data were elements C, O, N, and Cl with weight ratios of 93.15%, 3.12%, 1.76%, and 1.18%, respectively.

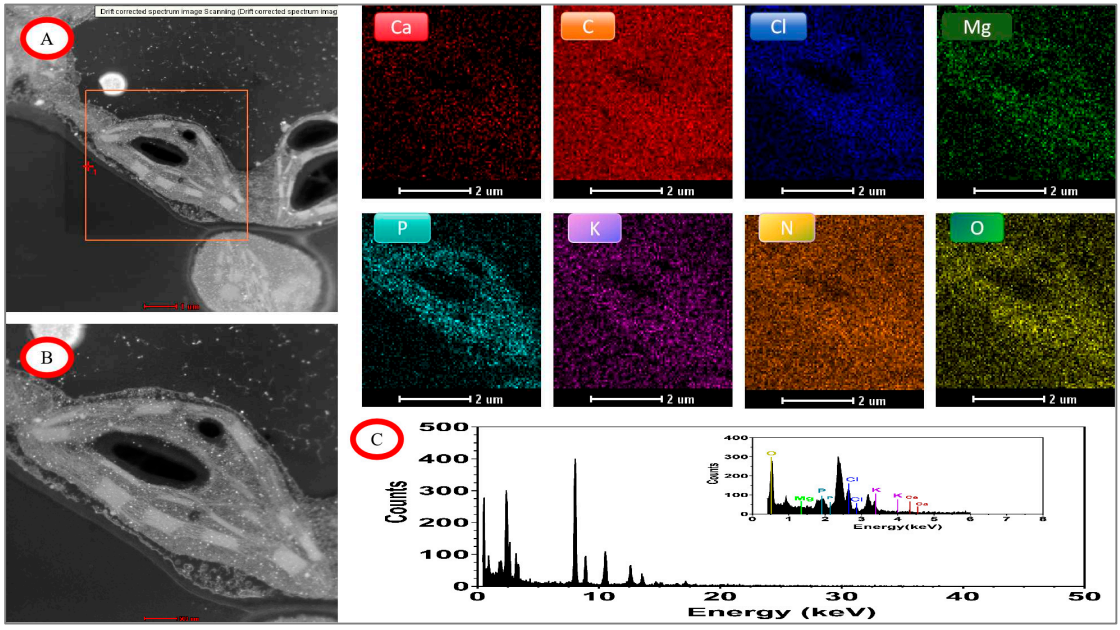

Preprints (www.preprints.org) | NOT PEER-REVIEWED | Posted: 18 January 2024 doi:10.20944/preprints202401.1427.v1

Figure 9. EDX mapping images of tomato chloroplasts under day/night temperature treatments of 25°C/15°C(CKT) with N3 treatment. A, drift corrected spectrum image Scanning; B, acquire high angle annular dark field image (HAADF); C, energy dispersive X-ray spectroscopy (EDX) of tomato chloroplasts; other image of Ca. C, Cl, Mg, P, K, N, O mapping area, scale bar, 2.0 μm.

Under high temperature treatment and low nitrogen treatment N2, the main distribution of C, N, O, P, Cl and Mg in chloroplasts and cell walls are as follows (Figure 10). There are obvious segmentation lines of Ca, P and Cl on both sides of the inner and outer chloroplasts, and they are enriched in the chloroplasts, which can outline the boundary of the chloroplasts. C and N elements are distributed throughout the scanning field. Through quantitative data analysis, the most abundant elements are C, O, N and Cl elements, with weight ratios of 90.82%, 4.85%, 1.96% and 1.24%, respectively.

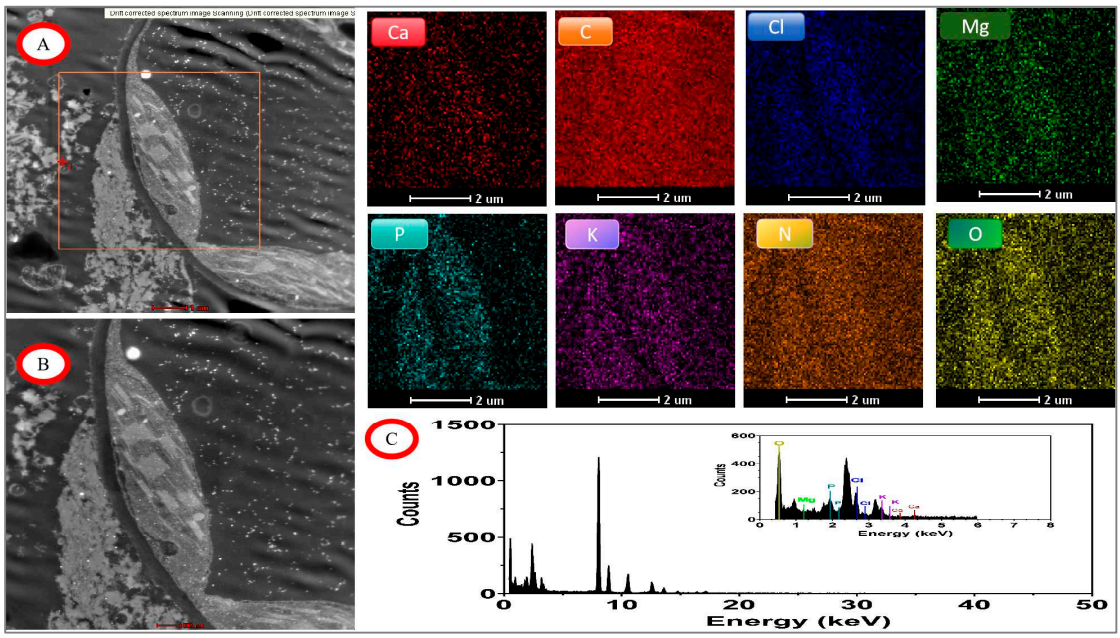

Figure 10. TEM-EDX mapping images of tomato chloroplasts under day/night temperature treatments of 40°C/30°C(HT) with N2 treatment. A, drift corrected spectrum image Scanning; B, acquire high angle annular dark field image (HAADF); C, energy dispersive X-ray spectroscopy (EDX) of tomato chloroplasts; other image of Ca. C, Cl, Mg, P, K, N, O mapping area, scale bar, 2.0 μm.

The main distributions of elements are C, N, O, P, Cl, and Mg in chloroplasts and cell walls under the high temperature treatment and the recommended nitrogen application rate of N3 (Figure 11). element P remained clearly segmented on the inner and outer sides of the chloroplasts and was enriched in the stroma and on the stroma-like cysts, which could outline the outer boundaries of the chloroplasts and the starch grains inside. elements Ca and Cl could distinguish the contours of the starch grains in the stroma bodies. The Ca and Cl elements can distinguish the outline of starch granules in amyloplasts, and the C and O elements are distributed throughout the scanning field of view, including the chloroplasts and the starch granules therein. By quantitative data analysis, the most abundant elements were C, O, N, and Cl, with weight ratios of 92.06%, 3.91%, 2.14%, and 1.36%, respectively.

Preprints (www.preprints.org) | NOT PEER-REVIEWED | Posted: 18 January 2024 doi:10.20944/preprints202401.1427.v1

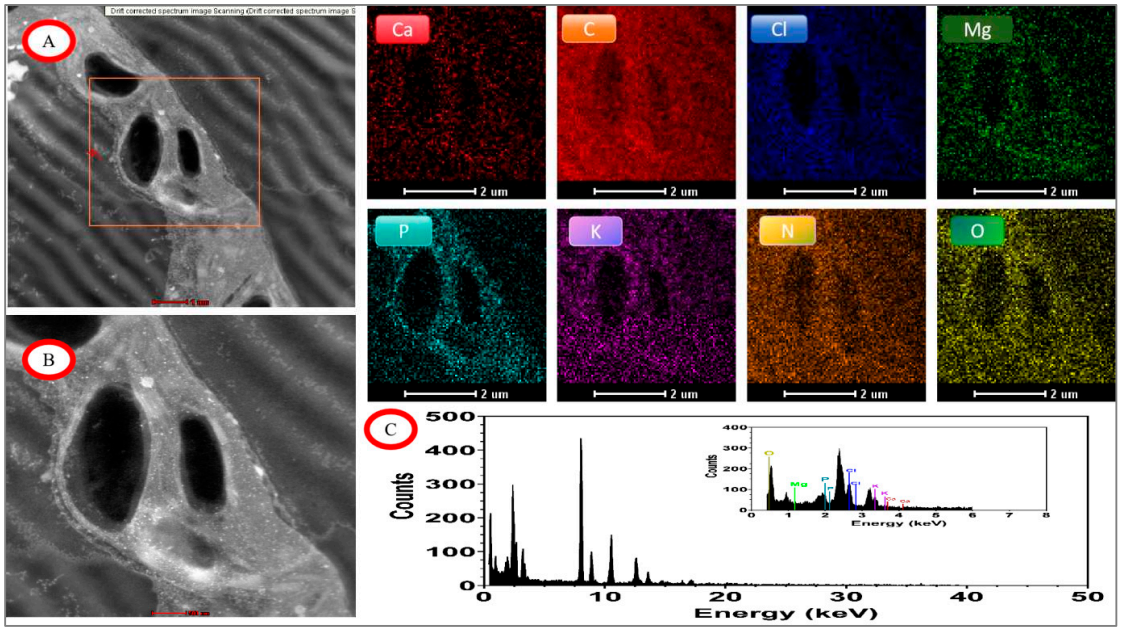

Figure 11. EDX mapping images of tomato chloroplasts under day/night temperature treatments of 40°C/30°C(HT) with N3 treatment. A, drift corrected spectrum image Scanning; B, acquire high angle annular dark field image (HAADF); C, energy dispersive X-ray spectroscopy (EDX) of tomato chloroplasts; other image of Ca. C, Cl, Mg, P, K, N, O mapping area, scale bar, 2.0 μm.

Under high temperature treatment and high nitrogen N4 treatment, the elements of Cl, Mg, and P were still distinctly segmented on both the inner and outer sides of the chloroplasts (Figure 12).The element P was enriched in the stroma of chloroplasts and on the cysts, which could distinguish the outer boundaries of the chloroplasts as well as the contours of the inner starch grains.The elements of C, N, and O were distributed in the entire scanning field of view that included the chloroplasts and starch grains in them. The most abundant elements analyzed by quantitative data were the elements C, O, N, and Cl with weight ratios of 90.62%, 3.93%, 3.03%, and 1.71%, respectively.

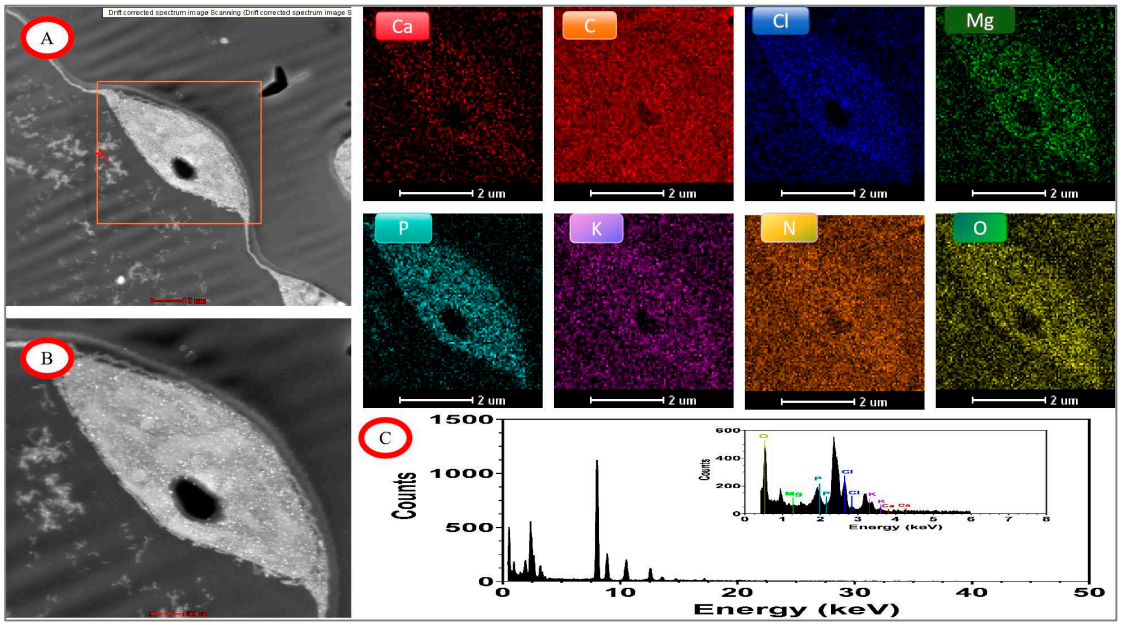

 doi:10.20944/preprints202401.1427.v1

Figure 12. EDX mapping images of tomato chloroplasts under day/night temperature treatments of 40°C/30°C(HT) with N4 treatment.. A, drift corrected spectrum image Scanning; B, acquire high angle annular dark field image (HAADF); C, energy dispersive X-ray spectroscopy (EDX) of tomato chloroplasts; other image of Ca. C, Cl, Mg, P, K, N, O mapping area, scale bar, 2.0 μm.

3. Discussion

Chloroplasts are the site of photosynthesis in plants. Maintaining the structural stability of chloroplasts is both expensive and complex because photosynthetic chemistry itself produces photo-oxidative damage. Under abiotic stresses such as heat stress, chloroplast degradation and cell death are mechanisms by which plants adapt to such stresses with a dual purpose: to protect cells and organs by removing reactive oxygen species-producing chloroplasts, and to redistribute nutrients to other tissues. However, the molecular mechanisms that initiate and promote this degradation are complex and involve multiple pathways. These pathways are all related to photosynthesis and nitrogen metabolism, so there is great potential to manipulate these pathways to improve crop yield and quality under heat stress environments. Little research has been done on nitrogen levels regulating the degradation of molecular structures within chloroplasts under heat stress.

3.1. Nitrogen levels changed the ultrastructure of tomato chloroplasts under heat stress

First, the degree of chloroplast differentiation increased at the onset of heat stress, which was higher in the low-nitrogen treatment than in the high-nitrogen treatment. The division of plastids started with the constriction in the middle of the plastid. As seen in Figure 13a-d, the dichotomy of chloroplasts was seen in the middle. The constriction becomes deeper and tighter, forming a very narrow isthmus before the two daughter cells are completely separated. The division mechanism consists of two constriction ring systems: an inner ring located on the matrix side of the inner pericycle and an outer ring formed on the cytoplasmic side of the outer pericycle. The inner ring subunit is thought to be a homolog of the FtsZ protein, which plays a role in cell division in cyanobacteria (thought to be endosymbiotic precursors of chloroplasts). The outer ring contains a polysaccharide ring composed of polyglucose chains and an associated dynamin. The dynamin proteins are composed of a mechanical protein, and they are also involved in the contractile ring of the lattice protein-encapsulated vesicle outgrowth, as well as in the formation of dumbbell-shaped vesicles assembled by the cell plate. Chloroplast division begins with the formation of the FtsZ ring, which recruits cytoplasmic glycosidyltransferases to the contractile site, producing polyglucose molecules that eventually form the polysaccharide ring; in turn, the polysaccharide ring serves as a template for the kinesin molecules that produce the contractile force.

The number of chloroplasts in the spongy tissue chloroplasts of tomato leaves observed by transmission electron microscopy at control temperature increased and then decreased with the increase of nitrogen application. The number of chloroplasts in cell of the leaf spongy tissue was the highest under the optimum nitrogen application rate N4. Under the high temperature treatment at 40°C, the number of chloroplasts increased more slowly with the increase of nitrogen application, and both were significantly smaller than the control temperature treatment.

Preprints (www.preprints.org) | NOT PEER-REVIEWED | Posted: 18 January 2024 doi:10.20944/preprints202401.1427.v1

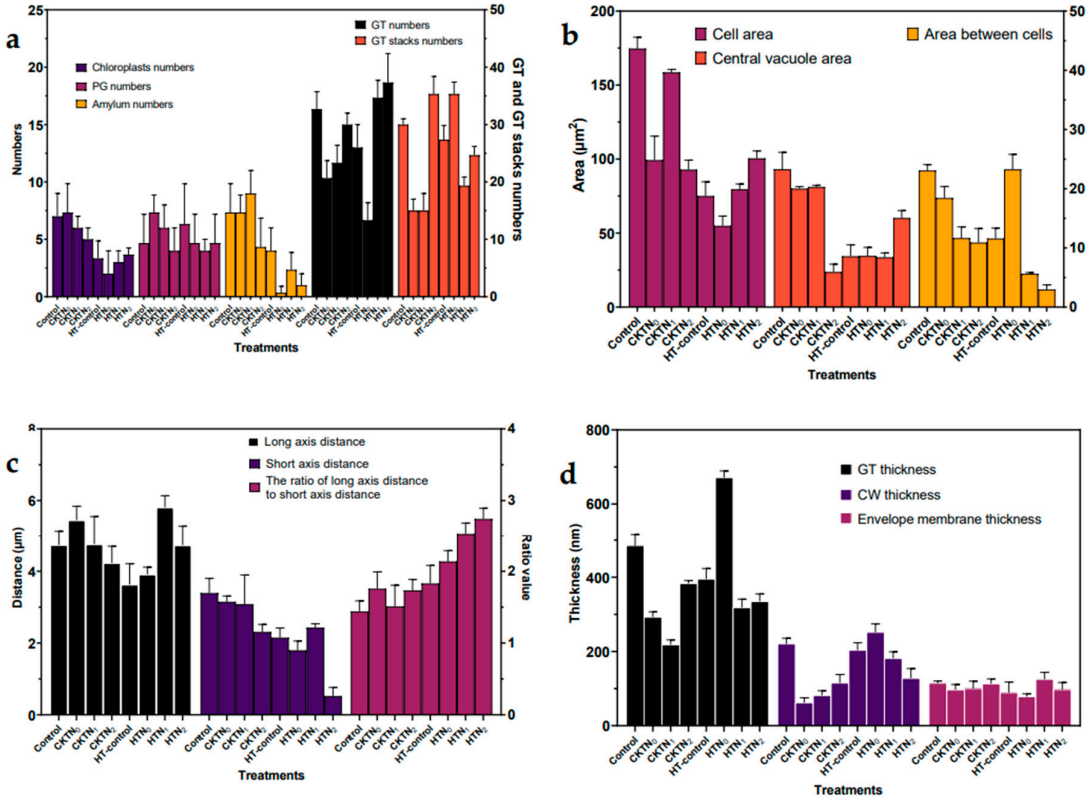

Figure 13. Ultrastructural parameters of tomato chloroplasts. a, numbers of chloroplasts, PG, GT, GT stack and amylum; b, area of cell, between cells and central vacuole; c, distance of chloroplast long axis and short axis, and the ratio of long axis distance to short axis distance; d, thickness of GT, CW and envelop membrane. PG, plastoglobuli; CW, cell wall; GT, grana thylakoid; ST,stroma thylakoid .

Second, the addition of N changes the morphology and distribution of certain genomes in the chloroplast. Many of the genes in the plastid genome form polycistronic transcriptional units, that is, two or more genes form a cluster and are transcribed by RNA polymerase from a single promoter. This is somewhat similar to prokaryotic manipulators; however, unlike prokaryotic manipulators, the plastid genome also contains polycistronic transcriptional units composed of functionally distinct genes. Typically, mRNAs for genes encoding photosynthetic proteins tend to be present in nonphotosynthetic plastids as well, such as pollen-forming bodies in roots and chloroplasts in tomato fruits. Apparently, these mRNAs are not translated into functional proteins. These findings illustrate the important role of posttranscriptional regulation in the regulation of plastid gene expression.

Third, the addition of nitrogen affected the structure of chloroplast-like vesicles. Photosystem I and the ATP synthase complex are present only in the unfastened regions of the stroma and stroma stacks. Photosystem II and light-trapping complex II are found mainly in the adherent regions of the stacked oocysts. This segregation of protein complexes between membranes on the adherent side of the stacked region and membranes on the unfastened side of the unstacked region is called lateral heterogeneity of the photosynthetic membrane system. The vesicle-like stacking structure is common in green plants and is thought to be involved in regulating the partitioning of absorbed light energy between photosystem I and photosystem II in photosynthesis. plastoglobuli are lipoproteasomes formed by a single layer of polar lipids surrounded and attached to the stromal side of the cystoid membrane. The lipid cores contain various types of isoprenylbenzoquinones [α-tocopherol (vitamin E), chlorophyll quinone (vitamin K1), plastoquinone, and methylnaphthoquinone], as well as the degradation products of carotenoids, neutral lipids, and chlorophyll. The boundary layer is composed of a monolayer of galectin glycerol, structural proteins called plastoglobulins, and enzymes involved in the synthesis and metabolism of core lipids. The size and number of

Preprints (www.preprints.org) | NOT PEER-REVIEWED | Posted: 18 January 2024 doi:10.20944/preprints202401.1427.v1

plastoglobulins change during plastid development and differentiation; the number of plastoglobulins becomes larger in response to environmental stresses (e.g., intense light, drought, high salt and high ozone environments) and during senescence.

3.2. Nitrogen levels correlate with changes in the spatial distribution and amounts of some elements in chloroplasts

Further analysis of EDX-mapping elements showed that nitrogen translocation to chloroplasts increased with increasing N application under high temperature stress, but carbon content decreased with increasing N application(Figure 14). The chloroplasts under low nitrogen treatment N2 had the highest amount of elemental oxygen and presumably the highest amount of carbon oxides (e.g., sugars such as starch). Oxygen elements in chloroplasts under the recommended nitrogen application N3 and high nitrogen N4 treatments, on the other hand, did not change significantly. This result suggests that excess nitrogen did not produce more sugars even though it was transported into the chloroplasts. Meanwhile, the content of P element in chloroplasts was higher under N2 treatment, and it was speculated that the excess nitrogen might be combined with P element to form phosphate-like compounds. Specific analyses are discussed below.

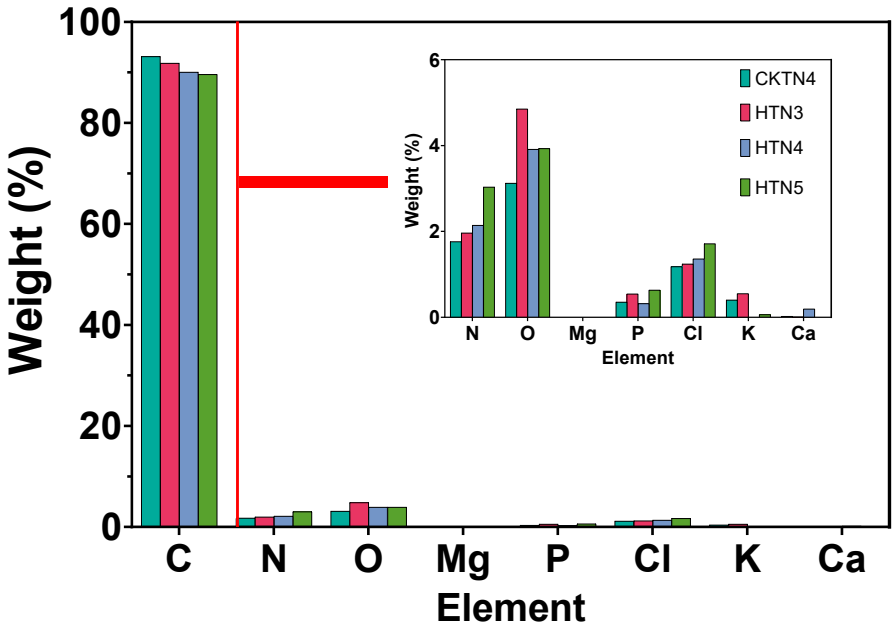

Figure 14. Quantitative data from EDX mapping elemental scans of tomato chloroplasts.

First, nitrogen levels correlate with P elements and alter the extent of starch breakdown and storage in chloroplasts under heat stress. Previours study showed that N level had no substantial effects on the deposition of starch, but altered the accumulation of protein, and the responses of protein accumulation to the effects of temperatur [28,29]. In contrast, we found that nitrogen levels affected the number, area, and morphological structure of starch grains in chloroplasts under 40 °C/30 °C high-temperature treatment. This may be related to the phosphorylation degradation process of starch. Elemental P, widely present on chloroplast-like vesicles and distinguishes the boundary between chloroplasts and other structures such as the cytoplasm and cell wall. The distribution on the stroma is significantly redundant with that of the stroma-like vesicles. The most obvious feature is that under heat stress, elemental P surrounds the starch granules in an encircling ring. Starch is the most prevalent form of carbohydrate storage in plants, and it accumulates in many different tissues and organs, including chloroplasts in leaf cells. The semi-crystalline lamellar structure of starch granules, which originates from the extrusion of adjacent double helical branched starch chains, creates a structure that is less likely to be attacked by starch-degrading enzymes [30].

Preprints (www.preprints.org) | NOT PEER-REVIEWED | Posted: 18 January 2024 doi:10.20944/preprints202401.1427.v1

The first step in starch degradation in chloroplasts is the phosphorylation of a small proportion of the glucose residues of branched-chain starch in the presence of two enzymes, including glucan, water dikinase (GWD) and phosphoglucan, water dikinase (PWD).GWD binds to the surface of the starch granule and introduces a phosphoryl group at the C-6 position of the glucose residue (reaction 1). PWD then binds to the phosphorylated starch and introduces another phosphorylated group at the C-3 position of the glucose residue (Reaction 2).

Reaction 1: GWD

$$1，4-\alpha-p-\text{Glucan}+\text{ATP}\rightarrow 1，4-\alpha-D-\text{Glucan}\ 6-P+P_i+\text{Maltose}$$

Reaction 2: PWD

$$1，4-\alpha-p-\text{Glucan}+\text{ATP}\rightarrow 1，4-\alpha-D-\text{Glucan}\ 3-P+P_i+\text{Maltose}$$

Phosphorylation changes the nature of the particle surface, with the hydrophilic phosphate group interrupting the arrangement of the double helix and destabilizing the double helix itself. This makes the exposed dextran chains more sensitive to a range of enzymes that can degrade glycosidic bonds. Carbon assimilation, which depends on ribulose-1, 5-bisphosphate carboxylase/oxygenase (Rusbiso), is one of the major place sensitive to heat stress in photosynthesis [31]. During heat stress, the degree of phosphorylation on the surface of starch granules in chloroplasts at different levels of nitrogen application could be obtained based on the quantitative analysis of phosphorus, HTN4>HTN2>control>HTN3. further quantitative analysis of C element could be obtained to show the change of starch content in chloroplasts, control>HTN3>HTN2>HTN4. both low nitrogen N2 treatment and high nitrogen N4 treatment changed the degree of phosphorylation on the surface of starch granules in chloroplasts, making the chloroplasts more sensitive to a range of enzymes that can degrade glycosidic bonds. The degree of phosphorylation on the surface led to an increase in the content of P element in chloroplasts. The increase in starch phosphate content and accelerated starch degradation can be indicated, leading to a low level of starch accumulation in the leaves, which ultimately led to a decrease in the dry matter accumulation of the leaves.

Second, nitrogen levels affect the spatial distribution and content of elemental Cl in chloroplasts. Elemental chlorine is absorbed by plants in the form of Cl^- and is mainly involved in photosynthesis in plants. In photosynthesis, chlorine participates in the photolytic water-oxygenation reaction of photosynthesis system II as a cofactor of the manganese-containing oxygen-excreting system. It helps to stabilize manganese ions in a higher oxidation state, and it also promotes photosynthetic phosphorylation. At the same time, chlorine accumulates preferentially in chloroplasts and plays a protective role in the stabilization of chlorophyll.

Multiple signaling pathways are present in the heat stress response, along with cross-linking in the oxidative stress response. Cytoplasmic H_2O_2 production is induced during heat stress and leads to cellular damage. Oxygen burst is associated with the expression of genes that cause heat stress induction, possibly as a result of direct perception of H_2O_2 by HSF. Other signaling molecules such as calcium ions are also involved. In the present study, calcium levels were found to be significantly elevated in passing. A great deal of research work still needs to be done on the perception, signaling process, regulatory network and how HSP recognizes target proteins for folding and degradation during heat stress. It is hoped that by combining the knowledge of crystallography with material science, the EDX mapping system equipped with transmission electron microscope can be used to further analyze the structural changes of molecules and constituent elements related to heat stress in chloroplasts at the nanometer scale.

Third, nitrogen levels affect the spatial distribution and content of elemental Ca in chloroplasts. Heat stress can lead to an imbalance in calcium ion homeostasis in plants, affecting plant growth and development. During photosynthesis, calcium ions can improve plant photosynthesis by maintaining the stability of its photochemical stages. It was found that under heat stress, the activity of the cystoid protein complex, which comprises the cystoid membrane structure, can be protected by calcium ions, resulting in enhanced activity of the membrane ATPase.

Therefore, under heat stress, calcium ions in chloroplasts may be involved in the plant's anti-stress response and have an effect on plant growth and photosynthesis.

 doi:10.20944/preprints202401.1427.v1

Besides, nitrogen levels affect the spatial distribution and content of elemental Mg in chloroplasts. Under heat stress, chloroplast magnesium ions may act through several mechanisms: 1. Stabilizing chloroplast structure: Magnesium ions are a component of chlorophyll in chloroplasts, and they may help maintain the structure and function of chloroplasts. Under heat stress, chloroplasts may be damaged, and the presence of magnesium ions can reduce this damage, thereby protecting the integrity of the chloroplasts. 2. Participation in photosynthesis: Photosynthesis is an important process in plant growth and development, and magnesium ion is one of the key elements in photosynthesis. Under heat stress, photosynthesis may be inhibited, and the presence of magnesium ions can help to maintain normal photosynthesis. 3. Regulation of ionic balance: Under heat stress, the ionic balance in plants may be disrupted, leading to changes in ion concentrations. Magnesium ions can interact with other ions to regulate the ionic balance, thus helping plants to adapt to the heat stress environment. 4. Antioxidant effect: Heat stress can lead to the production of large amounts of reactive oxygen species in plants, which can cause damage to plants. Magnesium ions can act as an antioxidant, scavenging reactive oxygen species from the body, thereby reducing damage to the plant. It is important to note that these mechanisms may not be independent of each other, but interact and influence each other. In addition, the mechanism of magnesium ion's action under heat stress needs to be confirmed by further studies.

The study of the regulatory role of nitrogen in combination with heat stress proteins and leaf senescence-regulated gene expression might be a future research direction. Many features of the plant response to chronic heat stress are conserved in all organisms. A typical response to acute heat stress is a rapid and transient reprogramming of gene expression, including a reduction in protein synthesis and an acceleration of transcription and translation of the heat shock protein (HSP), which functions primarily as a molecular chaperone and is involved in various aspects of birth protein folding and refolding of heat-denatured proteins. Based on their approximate molecular mass, HSP can be classified into five major groups: HSP100/Clp, whose main functions are protein depolymerisation, defolding, and degradation (Clp protease); HSP90, which promotes the maturation of signalling molecules, and genetic cushioning; HSP70, which prevents polymerisation, aids in refolding, protein trafficking, signalling, and transcriptional activation; and HSP60/Companion, which is an essential component of the HSP family of proteins, and is involved in all aspects of protein folding and heat-damaged protein refolding. The main functions of proteins are protein folding and helping refolding; the main functions of sHSP are preventing aggregation and stabilising proteins in their unnatural state. All five classes of HSP proteins are distributed in chloroplasts. Therefore, further analyses of the localisation of HSP proteins in chloroplasts are necessary in the future. Also , Some reports show that tomato SP1 and SPL2 regulate leaf senescence, revealing conserved functions of CHLORAD in plants [32].

In the future, the use of TEM-EDX mapping to analyse the ultrastructures and constituent elements of chloroplasts at the nanometer level, in combination with crystallographic theories in materials science and physical research methods [33,34], will further advance the analysis of molecular structures, including genome sequencing. However, quantification of energy-dispersive X-ray (EDX) spectra collected with a scanning transmission electron microscope (STEM) or transmission electron microscope (TEM) is usually performed using the Cliff-Lorimer or ζ-factor algorithms. Both algorithms depend upon the comparison of the measured spectra with spectra collected from thin-film standards. Furthermore, the availability of thin-film standards is very limited due to the many challenges in their fabrication and characterization [35].

4. Materials and Methods

2.1. The Plant materials and growth conditions

The experiment was conducted in the Venlo-type greenhouse (roof height × shoulder height × width × length, 5.0 × 4.5 × 9.6 × 30.0 m) of Jiangsu Key Laboratory of Agricultural Meteorology of Nanjing University of Information Science and Technology from March 2022 to August 2022. Tomato seedlings (*Lycopersicon esculentum* Mill., Caesar) were planted into flowerpots of size 30 cm (height)

 doi:10.20944/preprints202401.1427.v1

× 30 cm (upper diameter) × 25 cm (bottom diameter) filled with peat soil: perlite: vermiculite = 2:1:1(v/v/v). The tested soil was medium loam, with uniform soil fertility, pH value of 7.4.

Experiments design temperature and nitrogen two factors for a duration of 5 days. The temperature is set at two levels, with day/night temperatures of 25°C/15°C(CKT) and 40°C/30°C (HT). The four levels of nitrogen (urea, 46% N) were 0.0 kg hm^{-2}(N1), 187.5 kg hm^{-2}(N2), 250 kg hm^{-2}(N3, as recommended nitrogen-application), and 312.5kg hm^{-2} (N4). The proportion of nitrogen applied at seedling, flowering and fruiting, green ripening and color change stages was 30%: 30%: 20%: 20%, respectively. All seedlings were divided into 8 groups of 9 pots each. Plants that absorbed nitrogen after 5 days were moved into an artificial climate chamber (BDW 40, Conviron, Canada). During the treatments, relative humidity was set at 50 to 80%, light hours were from 6:00 to 18:00 (daytime), and photosynthetically active radiation ranged from 0 to 1000 μmol m^{-2} s^{-1}.

During the treatment period, three pots of tomatoes were selected and sampled on the 2nd to 3rd functional leaf from the top of the tomato. A total of 24 samples were taken in three replications. Water was supplied twice daily during the treatment period. All plants were irrigated up to 80% of field capacity (monitored by soil moisture content tester) to avoid water deficit. At the end of the treatment, all plants were moved to a Venlo-type greenhouse for recovery.

2.2. Transmission electron microscopy of tomato leaves

The tomato leaf transmission electron microscopy sample preparation was referred to the observation method of Zhou et al. [36], combined with my previous experience in scanning electron microscopy sample preparation (Figure 15). Sample preparation for ultrathin sectioning and transmission electron microscopy photography were entrusted to Zhenjiang Zhuanbo Inc(Danyang, China). The specific process is summarized as follows:

(1) Sampling. Wash the leaf surface spoils with water before sampling. Avoiding the main leaf veins, use a surgical scalpel to cut a leaf tissue block of less than 3 mm. Then quickly put into 2.5% glutaraldehyde fixative.

(2) Fixation. Plant samples were immersed in 3% glutaraldehyde fixative configured with 0.1 mol/L PBS buffer (pH 6.8~7.2) for 1~2h at room temperature, and pumped to make the samples sink to the bottom of the tube. Vigorous oscillation during the period caused the air bubbles to detach from the sample and ensured that the sample was always in the fixative. Replace the 2.5% glutaraldehyde fixative configured with 0.1 mol/L PBS buffer (pH 6.8~7.2), and fix overnight at 4℃.

(3) Rinsing. Fill the centrifuge tube with 0.1 mol/L PBS buffer (pH 6.8~7.2) and rinse 3 times for 15 min each time. shake continuously during the period to make the rinsing sufficient.

(4) Post-fixation. The samples were immersed in 10g/L osmium tetroxide fixative configured in 0.1 mol/L PBS buffer (pH 6.8~7.2) for 2h at room temperature until the samples turned black.

(5) Rinsing. Fill the centrifuge tube with 0.1 mol/L PBS buffer (pH 6.8~7.2) and rinse 3 times for 15 min each time.Shake continuously during the period to make the rinsing sufficient.

(6) Gradient dehydration. Dehydrate with 50%, 70%, 80%, 90%, 95% ethanol, respectively, each time 15min. 100% ethanol dehydration 2 times, each time 20min. finally, replace with 100% acetone 2 times, each time 20min.

(7) Permeabilization and embedding. Pure acetone: Spurr embedding agent 3:1:1 mixture were infiltrated for 1h, pure acetone: Spurr embedding agent 1:3 mixture infiltrated for 3h, and then the sample with a toothpick to pick out, on filter paper to absorb the dryness of the sample into a clean centrifugal tube, add pure Spurr embedding agent infiltration for more than 12h. Then pure embedding agent was added to a 0.5mL sharp-bottomed centrifuge tube, and air bubbles were driven out with a toothpick. The sample was picked into the mold and adjusted to the proper orientation. Place a piece of label paper with the name of the sample into the mold together and cover with a lid to isolate the adverse effects of oxygen on the polymerization of the Spurr embedding agent. Put into the 70 ℃ oven polymerization more than 8h.

(8) Half package slice positioning. Polymerization completed embedded block with a toothpick poke to see if there are traces, if not, it means that the hardness to meet the requirements. Embedded block will be removed from the mold, clamped with a fixture to repair the block. Trim off the excess

Preprints (www.preprints.org) | NOT PEER-REVIEWED | Posted: 18 January 2024 doi:10.20944/preprints202401.1427.v1

resin around the perimeter of the sample with a double-sided blade and correct the cut surface flush with a glass cutter (until it reflects the reflection). A water trough was made in the newly made glass knife, and semi-thin sections were made with this knife, fished onto slides, and heated and baked to dry the water so that the sections were flat against the slide. Stained with 20 g/L toluidine blue for a few minutes, washed and dried and observed under a light microscope to find where the study object was located and to determine the orientation of the section.

(9) Ultrathin section. The sample block was then trimmed again based on this location information, cutting the excess sample and trimming the cut surface until it was flat and smooth, leaving only a small area where the study object was located to reduce the difficulty of ultra-thin sectioning. Ultrathin sectioning was performed with a diamond knife or glass knife, and the thickness was controlled at 70~100 nm. The ultrathin sections were sliced on a coated copper mesh, and the excess water was drained off and set aside.

(10)Electronic staining. Ultrathin sections were stained with uranyl acetate for 10~15min, and the staining was carried out in an air-insulated apparatus to eliminate the interference of moisture and carbon dioxide, and an appropriate amount of sodium hydroxide could be added to the side of the block to absorb the moisture and carbon dioxide from the environment of the apparatus to ensure that the samples were free from lead contamination; the samples were washed with double-distilled water for three times, and then dried naturally before being subjected to transmission electron microscopy observation.

(11)The samples were observed and photographed with an HT7800 transmission electron microscope (Hitachi, Japan).

Figure 15. Transmission electron microscopy and photographs of experimental procedure.

2.3. X-ray energy spectroscopy of thin samples of chloroplasts from tomato leaves

(1) Quantitative analysis principle of X-ray energy spectrometry analysis

According to the continuous spectroscopy method developed by Hall et al. The main principle of this method is that the concentration C_x of an element X within the sample is directly proportional to the count rate of the characteristic peaks of that element, which is calculated by the formula:

$$C_x = \mathrm{k}(p - b)/(\mathrm{W_t} - \mathrm{W_b}) \qquad (1)$$

where is the concentration of an element within the sample; k is the coefficient value of each element, determined by analyzing the specimen; p is the back-bottom count rate of the element; is the total

 doi:10.20944/preprints202401.1427.v1

count rate of the continuous spectrum; and is the count rate emitted from the external source (supporting membrane, grid, etc.) within the continuous spectrum.

This leads to the formula for the quantification of the element in biological thin-labeled samples:

$$C_x = \frac{I_x/I_b}{I_s/I_{sb}} C_s \frac{G_x}{G_x} \quad (2)$$

where is the concentration of the element under test in the sample; is the concentration of the element in the specimen; is the measured intensity of the characteristic X-rays of the element in the sample; is the measured intensity of the continuous X-rays of the element in the sample; and is the measured intensity of the characteristic X-rays and continuous X-rays of the element in the specimen; and is the elemental factor of the chemical composition of the sample and the specimen, respectively, (also known as the G-factor).The G-factor can be calculated by the following equation The G-factor can be calculated by the following equation:

$$\mathrm{G} = \sum_{1}^{\mathrm{n}} \mathrm{C_i Z_i^2 / A_i} \quad (3)$$

where is the percentage of element i in the chemical composition of the thin sample or thin specimen; is the atomic number of element i; is the atomic weight of element i; and n is the constituent element of the sample.. The specific energy fluxes were calculated by following equations.

2.4. Statistical Analysis

Data were plotted and analyzed using Graphpad Prism version 9.5.0 for Windows, Graphpad Software, San Diego, California USA,. Cell statistics and analysis were performed using Fiji ImageJ software(https://imagej.net/imagej-wiki-static/Fiji/Downloads). SPSS Statistics 26(SPSS, Chicago, IL, USA) was used to analyse the differences in the data, and Duncan's test was performed for multiple comparisons (α = 0.05).

5. Conclusions

In summary, appropriate nitrogen application level can alleviate the damage of heat stress to the ultrastructure of tomato chloroplasts and mapping elements, and improve the photosynthetic capacity of tomato plants, thereby enhancing their heat tolerance. However, excessive nitrogen application may also have adverse effects on tomato growth and development, so it is necessary to control the application amount of nitrogen reasonably.

6. Patents

A method and system for detecting factors affecting tomato growth and quality under high temperature stress. China patent. CN115032219A.

Author Contributions: Conceptualization, C. L. and Z. Y.; methodology, Z. Y.; software, C. Z. and C. L.; validation, C. Z. and Z. Y.; formal analysis, C. L. and C. Z.; investigation, Z. Y. and C. L.; resources, C. L.; data curation, C. L. and J. L.; writing—original draft preparation, C. L. and C. Z.; writing—review and editing, C. L. and Y. Y.; visualization, C. L., D. W. and C. Z.; supervision, Z. Y. and C. Z.; project administration, Z. Y.; funding acquisition, C. Z.. All authors have read and agreed to the published version of the manuscript.

Funding: This research was funded by Natural Science Research Program of West Anhui University, grant number WXZR202212, High-level talent scientific research star-up project of West Anhui University, grant number WGKQ2021045, and Open Project of Anhui Forest Crop Intelligent Equipment Engineering Research Center, grant number AUCIEERC-2022-03.

Data Availability Statement: The data used to support the findings of this study are available from the first and corresponding author upon request.

Acknowledgments: We thank the anonymous reviewers for their constructive comments and suggestions on revising the manuscript. Special thanks to Mr. Zhou Weidong, General Manager of Zhenjiang Zhuanbo Inspection Technology Co., Ltd. for his technical support and guidance during the transmission electron microscopy samples and photographing process.

Conflicts of Interest: The authors declare no conflicts of interest.

References

1. N. BERTIN, Analysis of the Tomato Fruit Growth Response to Temperature and Plant Fruit Load in Relation to Cell Division, Cell Expansion and DNA Endoreduplication, Annals of Botany, Volume 95, Issue 3, February 2005, Pages 439–447, https://doi.org/10.1093/aob/mci042.
2. Fang Xiao, Zaiqiang Yang, Wei Han, Yongxiu Li, Yixuan Qiu, Qing Sun & Fangmin Zhang (2018) Effects of day and night temperature on photosynthesis, antioxidant enzyme activities, and endogenous hormones in tomato leaves during the flowering stage, The Journal of Horticultural Science and Biotechnology, 93:3, 306-315, DOI: 10.1080/14620316.2017.1369171.
3. Alsamir M, Mahmood T, Trethowan R, et al. An overview of heat stress in tomato (*Solanum lycopersicum* L.). Saudi journal of biological sciences, 2021, 28(3): 1654-1663. https://doi.org/10.1016/j.sjbs.2020.11.088.
4. Allakhverdiev S I，Kreslavski V D，Klimov V V，Los D A，Carpentier R，Mohanty P. 2008. Heat stress：An overview of molecular responses in photosynthesis. Photosynthesis Research 2008, 98 (1-3):541-550. https://doi.org/10.1007/s11120-008-9331-0.
5. Naiyao M D. 2016. Mitigation effect and physiological mechanism of nitrogen fertilizer on high temperature stress in the early stage of grain filling in rice. PhD Thesis, Nanjing Agricultural University, China.
6. Motamedi, E., Safari, M. & Salimi, M. Improvement of tomato yield and quality using slow release NPK fertilizers prepared by carnauba wax emulsion, starch-based latex and hydrogel nanocomposite combination. Sci Rep 13, 11118 (2023). https://doi.org/10.1038/s41598-023-38445-7.
7. Marchiori, P. E., Machado, E. C., & Ribeiro, R. V. (2014). Photosynthetic limitations imposed by self-shading in field-grown sugarcane varieties. Field Crops Research, 155, 30-37. https://doi.org/10.1016/j.fcr.2013.09.025.
8. Theobald, J. C., Mitchell, R. A., Parry, M. A., & Lawlor, D. W. (1998). Estimating the excess investment in ribulose-1, 5-bisphosphate carboxylase/oxygenase in leaves of spring wheat grown under elevated CO2. Plant Physiology, 118(3), 945-955.
9. LAZA, R. C., BERGMAN, B., & VERGARA, B. S. (1993). Cultivar differences in growth and chloroplast ultrastructure in rice as affected by nitrogen. Journal of Experimental Botany, 44(11), 1643-1648.
10. REBECCA C. LAZA, BIRGITTA BERGMAN, BENITO S. VERGARA, Cultivar Differences in Growth and Chloroplast Ultrastructure in Rice as Affected by Nitrogen, Journal of Experimental Botany, Volume 44, Issue 11, November 1993, Pages 1643–1648, https://doi.org/10.1093/jxb/44.11.1643.
11. Li, C.; Yang, Z.; Zhang, C.; Luo, J.; Zhang, F.; Qiu, R. Effects of Nitrogen Application in Recovery Period after Different High Temperature Stress on Plant Growth of Greenhouse Tomato at Flowering and Fruiting Stages. Agronomy 2023, 13, 1439. https://doi.org/10.3390/agronomy13061439.
12. Zahedi, M., McDonald, G., & Jenner, C. F. (2004). Nitrogen supply to the grain modifies the effects of temperature on starch and protein accumulation during grain filling in wheat. Australian Journal of Agricultural Research 2004, 55(5), 551-564.
13. Li, C.; Yang, Z.; Zhang, C.; Luo, J.; Jiang, N.; Zhang, F.; Zhu, W. Heat Stress Recovery of Chlorophyll Fluorescence in Tomato (Lycopersicon esculentum Mill.) Leaves through Nitrogen Levels. Agronomy 2023, 13, 2858. https://doi.org/10.3390/agronomy13122858.
14. Bassi, D., Menossi, M. & Mattiello, L. Nitrogen supply influences photosynthesis establishment along the sugarcane leaf. Sci Rep 8, 2327 (2018). https://doi.org/10.1038/s41598-018-20653-1.
15. Jensen PE, Leister D. Chloroplast evolution, structure and functions. F1000Prime Rep. 2014 Jun 2;6:40. doi: 10.12703/P6-40. PMID: 24991417; PMCID: PMC4075315.
16. Rasmussen, M., & Minteer, S. D. (2014). Thylakoid direct photobioelectrocatalysis: utilizing stroma thylakoids to improve bio-solar cell performance. Physical Chemistry Chemical Physics, 16(32), 17327-17331. https://doi.org/10.1039/C4CP02754J.
17. Henrysson, T., Sundby, C. Characterization of photosystem II in stroma thylakoid membranes. Photosynth Res 25, 107–117 (1990). https://doi.org/10.1007/BF00035459.
18. Bos, P., Berentsen, J., & Wientjes, E. (2023). Expansion microscopy resolves the thylakoid structure of spinach. Plant Physiology. https://doi.org/10.1093/plphys/kiad526.
19. Bertram Daum, Werner Kühlbrandt, Electron tomography of plant thylakoid membranes, Journal of Experimental Botany, Volume 62, Issue 7, April 2011, Pages 2393–2402, https://doi.org/10.1093/jxb/err034.
20. Opatíková, M., Semchonok, D.A., Kopečný, D. et al. Cryo-EM structure of a plant photosystem II supercomplex with light-harvesting protein Lhcb8 and α-tocopherol. Nat. Plants 9, 1359–1369 (2023). https://doi.org/10.1038/s41477-023-01483-0.
21. Harris, D., Toporik, H., Schlau-Cohen, G.S. et al. Energetic robustness to large scale structural fluctuations in a photosynthetic supercomplex. Nat Commun 14, 4650 (2023). https://doi.org/10.1038/s41467-023-40146-8.

22. Zhukov, A.; Popov, V. Eukaryotic Cell Membranes: Structure, Composition, Research Methods and Computational Modelling. Int. J. Mol. Sci. 2023, 24, 11226. https://doi.org/10.3390/ijms241311226.
23. Puppala N, Nayak SN, Sanz-Saez A, et al. Sustaining yield and nutritional quality of peanuts in harsh environments: Physiological and molecular basis of drought and heat stress tolerance. Frontiers in Genetics. 2023 ;14:1121462. DOI: 10.3389/fgene.2023.1121462. PMID: 36968584; PMCID: PMC10030941.
24. Tracey Ruhlman, Dheeraj Verma, Nalapalli Samson, Henry Daniell, The Role of Heterologous Chloroplast Sequence Elements in Transgene Integration and Expression, Plant Physiology, Volume 152, Issue 4, April 2010, Pages 2088–2104, https://doi.org/10.1104/pp.109.152017.
25. Kaur, H., Kaur, H., Kaur, H. et al. The beneficial roles of trace and ultratrace elements in plants. Plant Growth Regul 100, 219–236 (2023). https://doi.org/10.1007/s10725-022-00837-6.
26. Singhal, R.K., Fahad, S., Kumar, P. et al. Beneficial elements: New Players in improving nutrient use efficiency and abiotic stress tolerance. Plant Growth Regul 100, 237–265 (2023). https://doi.org/10.1007/s10725-022-00843-8.
27. Minenkov, A., Mörtlbauer, T., Arndt, M., Hesser, G., Angeli, G., & Groiss, H. (2023). Towards a dependable TEM characterization of hot-dip galvanized steels with low and high Si content. Materials & Design, 227, 111684.https://doi.org/10.1016/j.matdes.2023.111684.
28. Lihua Ning, Yuancong Wang, Xi Shi, Ling Zhou, Min Ge, Shuaiqiang Liang, Yibo Wu, Tifu Zhang, Han Zhao, Nitrogen-dependent binding of the transcription factor PBF1 contributes to the balance of protein and carbohydrate storage in maize endosperm, The Plant Cell, Volume 35, Issue 1, January 2023, Pages 409–434, https://doi.org/10.1093/plcell/koac302.
29. Ru, C., Wang, K., Hu, X. et al. Nitrogen Modulates the Effects of Heat, Drought, and Combined Stresses on Photosynthesis, Antioxidant Capacity, Cell Osmoregulation, and Grain Yield in Winter Wheat. J Plant Growth Regul 42, 1681–1703 (2023). https://doi.org/10.1007/s00344-022-10650-0.
30. Woodson, J. D. (2022). Control of chloroplast degradation and cell death in response to stress. Trends in Biochemical Sciences. https://doi.org/10.1016/j.tibs.2022.03.010.
31. Guodong Wang, Fanying Kong, Song Zhang, Xia Meng, Yong Wang, Qingwei Meng, A tomato chloroplast-targeted DnaJ protein protects Rubisco activity under heat stress, Journal of Experimental Botany, Volume 66, Issue 11, June 2015, Pages 3027–3040, https://doi.org/10.1093/jxb/erv102.
32. Ling, Q., Sadali, N.M., Soufi, Z. et al. Publisher Correction: The chloroplast-associated protein degradation pathway controls chromoplast development and fruit ripening in tomato. Nat. Plants 7, 1433 (2021). https://doi.org/10.1038/s41477-021-01018-5.
33. Karam, S.T.; Abdulrahman, A.F. Green Synthesis and Characterization of ZnO Nanoparticles by Using Thyme Plant Leaf Extract. Photonics 2022, 9, 594. https://doi.org/10.3390/photonics9080594.
34. Lomelí-Rosales, D.A.; Zamudio-Ojeda, A.; Reyes-Maldonado, O.K.; López-Reyes, M.E.; Basulto-Padilla, G.C.; Lopez-Naranjo, E.J.; Zuñiga-Mayo, V.M.; Velázquez-Juárez, G. Green Synthesis of Gold and Silver Nanoparticles Using Leaf Extract of Capsicum chinense Plant. Molecules 2022, 27, 1692. https://doi.org/10.3390/molecules27051692.
35. Makarem, R. (2019). Development of advanced Transmission Electron Microscopy techniques for nanoscale map** (Doctoral dissertation, Université Paul Sabatier-Toulouse III).
36. Zhou, T. Li, M. Peydayesh, M. Usuelli, V. Lutz-Bueno, J. Teng, L. Wang, R. Mezzenga, Oat Plant Amyloids for Sustainable Functional Materials. Adv. Sci. 2022, 9, 2104445. https://doi.org/10.1002/advs.202104445.